

## Miniband formation in asymmetric double-quantum-well superlattice structures

S. Fafard, Y. H. Zhang,\* and J. L. Merz

Center for Quantized Electronic Structures (QUEST), University of California, Santa Barbara, California 93106

(Received 5 May 1993)

We report on a type of semiconductor quantum structure that combines the sharp optical properties of multiple quantum wells and the transport properties of superlattices. By using coupled asymmetric double quantum wells built with a narrow well having a single bound electron state resonant with an excited state of a wider well, miniband formation is achieved through the hybridized extended states resulting from these overlapping wave functions, but the ground states of the wide wells remain localized as in the case of multiple quantum wells.

The steplike density of states obtained by confining carriers to two dimensions gives sharper optical properties to semiconductor multiple-quantum-well (MQW) structures, but also limits the transport properties in the direction of the confinement. A compromise can be obtained with superlattices (SL's), where one can tune the mobility perpendicular to the confining layers at the cost of a smoother onset of the optical absorption.<sup>1</sup> Practical devices based on intersubband transitions (such as infrared detectors) have used SL's with one miniband and the continuum states, or two minibands, to transport the photocreated carriers.<sup>2</sup> Even though these "regular" SL's, built with symmetric wells, are perhaps the simplest conceptually, they do not offer any freedom for individual tailoring of the coupling of the multiple bound states. Such minibandwidth engineering would be desirable (e.g., to reduce the dark current in infrared detectors), and can be achieved with the new asymmetric double-quantum-well superlattice (ADQWSL) structures we discuss in this paper.<sup>3</sup> Analogous to the alloying of a III and a V semiconductor, "alloying" of a narrow well (NW) and a matching wide well (WW) will form hybridized energy levels with constituent ground and excited states. More complicated structures combining two segments of SL's and requiring usage of a nested effective-mass approximation have been the subject of a theoretical investigation.<sup>4</sup> Also, structures coupling barrier SL's and single quantum wells (SQW's) gave enhanced intersubband absorption.<sup>5</sup> However, our ADQWSL is easily understood from the properties of the isolated NW's and WW's which constitute the asymmetric coupled double quantum wells (ACDQW's), and does not require thicker SL barriers. ACDQW's constructed with two wells having nonresonant levels have been studied with and without an applied electric field bringing their energy levels into resonance.<sup>6-9</sup> However, no study has been done on ACDQW structures having energy levels resonant in the flat band condition and/or having multiple ACDQW's coupled together through thin barriers. In addition, our ADQWSL will not suffer from the large blueshift of its ground states caused by the Wannier-Stark effect<sup>10</sup> which destroys the ground-state miniband of regular SL's, and is therefore particularly appropriate to combine optical absorption and transport under applied electric field. Moreover, the study of ADQWSL structures may help understanding of the physics of spatially indirect excitons and localized-

to-extended transitions,<sup>11</sup> and also give information on band nonparabolicity and band offset, as the resonance condition is sensitive to these parameters.<sup>12</sup>

The ADQWSL structure described here consists of ACDQW's having the same potential depth ( $V$ ); the resonance condition is thus achieved by tuning the well widths ( $L_{NW}$  and  $L_{WW}$ ) such that the ground state of the NW and an excited state in the WW are degenerate. Let us first consider the model of a NW with a single bound (electron) level resonant with the excited state of the two-level WW. The possible range for the energy level and the ratio of the well widths is determined from the eigenstate conditions:<sup>13</sup>  $0.54 \times V \leq E \leq V$  and  $L_{WW} = \alpha_2 L_{NW}$ . Similarly, for resonance with the second excited state of a three-level WW,  $0.65 \times V \leq E \leq V$ , and  $L_{WW} = \alpha_3 L_{NW}$ , where

$$\alpha_2 = \frac{\tan^{-1}(-1/\beta) + \pi}{\tan^{-1}(\beta)}, \quad \alpha_3 = \frac{\tan^{-1}(\beta) + \pi}{\tan^{-1}(\beta)}, \quad (1)$$

and  $\beta = [m_w^*/m_b^*(V/E - 1)]^{1/2}$ . Using Eqs. (1) the value of  $E/V$  can be chosen to obtain an acceptable ratio  $L_{WW}/L_{NW}$ , and the desirable energy spacing between the ground states localized in the WW's and the extended states forming the miniband through the ground states of the NW's and the excited states in the WW's. To evaluate the degree of localization of the nonresonant levels and the width of the miniband, the wave function and the probability densities were calculated. For example, see Fig. 1 for the case where  $E = 0.7 \times V$ ,  $\alpha_2 = 3.7$ , and  $\alpha_3 = 6.4$ , and  $V = 212$  meV, for a "regular" SL with five identical wells [Fig. 1(a)] and for ADQWSL's with the ground state in the NW ( $E_{NW}^1$ ) resonant with the first ( $E_{WW}^2$ ), and the second ( $E_{WW}^3$ ) excited state in the WW, in Figs. 1(b) and 1(c), respectively. The number of wells in the calculation can easily be increased, but it was found that five wells is more than sufficient to determine the interwell coupling and hence the minibandwidth (about 30 meV in all the above cases). It is also clear from Fig. 1 that, locally, the wave functions retain the symmetry of their respective wells, and therefore selection rules of the constituent SQW's are expected to prevail for the ADQWSL transitions. However, a single state in the middle of the miniband (near the energy of the isolated well, or equivalently when the SL wave vec-

tor equal  $\pi/2$ ) is an exception to the above rule, as it has the probability distribution in the WW's of the preceding state. Note the (weak) single hump in the WW's for the midstate of Fig. 1(b) (the effect is enhanced for thinner barrier). The calculated probability densities for the ADQWSL structure at the  $E_1^{\text{WW}}$  energy (not shown) demonstrate that these levels are localized in the WW just as if the NW and the two barriers are replaced by a continuous barrier of equal thickness (e.g., a 5.5-nm barrier + 2.25-nm NW + 5.5-nm barrier  $\approx$  13.25-nm barrier). Calculations with an electric field show that at a field exceeding  $\approx 20$  kV/cm the miniband of the ADQWSL structure has collapsed into a series of energy levels localized in the uncoupled biased wells, leading to the Wannier-Stark effect.

$\text{Al}_x\text{Ga}_{1-x}\text{As}/\text{GaAs}$  structures were grown by molecular-beam epitaxy on a  $n^+$  GaAs(100) substrate. Sample 1 has  $x=0.291$ ,  $L_{\text{NW}}=1.84$ , and  $L_{\text{WW}}=7.5$  nm, and a barrier thickness of  $d=4.1$  nm. A 100-nm  $\text{Al}_x\text{Ga}_{1-x}\text{As}$  barrier layer was grown on a 400-nm GaAs buffer layer, and then a 15-period stack of NW/barrier/WW/barrier was grown and capped with a NW, a 80-nm  $\text{Al}_x\text{Ga}_{1-x}\text{As}$  barrier, and a 20-nm GaAs

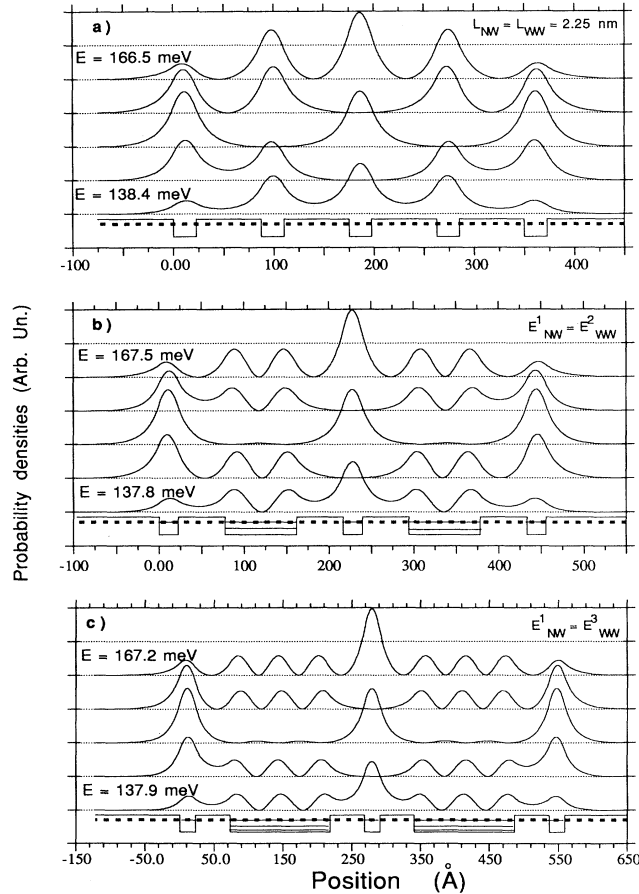


FIG. 1. The five electron energy levels contributing to the miniband formation in the case of (a) “regular” SL with five identical wells ( $L_{\text{NW}}=L_{\text{WW}}=2.25$  nm,  $d=6.5$  nm), (b) an ADQWSL with  $E_{\text{NW}}^1=E_{\text{WW}}^2$  ( $L_{\text{NW}}=2.25$ ,  $L_{\text{WW}}=8.4$  nm,  $d=5.5$  nm), and (c) an ADQWSL with  $E_{\text{NW}}^1=E_{\text{WW}}^3$  ( $L_{\text{NW}}=2.25$ ,  $L_{\text{WW}}=14.6$  nm,  $d=5.0$  nm).

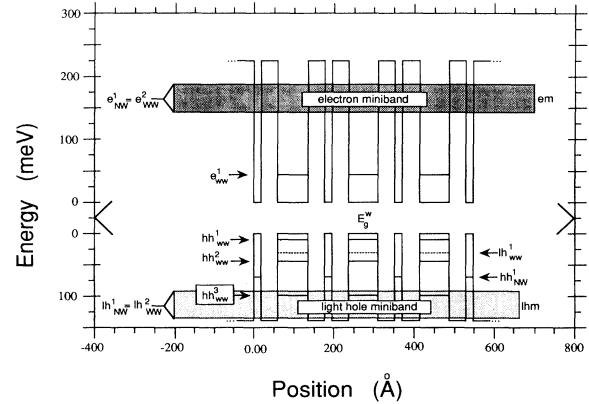


FIG. 2. Band diagram and energy levels for sample 1.

layer (as deduced from the growth parameters and optical spectra). Calculations show that the electron ground state in the NW ( $e_{\text{NW}}^1$ ) and the first excited state of the WW ( $e_{\text{WW}}^2$ ) are off-resonance by only 4 meV. Such a small difference (comparable with the energy difference induced by the well width fluctuations in the regular SL) is not expected to have much influence on the miniband formation as the expected miniband width for that structure is expected to be more than ten times larger (44 meV). Figure 2 depicts the band diagram and the resulting energy levels of ADQWSL sample 1, with the electron miniband (em), the localized energy levels  $e_{\text{WW}}^1$ ,  $lh_{\text{WW}}^1$  (light-hole ground state in the WW), etc., and also a light-hole miniband (lhm).

The quality of the ADQWSL sample is reflected by the predominance of the sharp [full width at half maximum (FWHM) smaller than 3 meV at low excitation intensity] photoluminescence (PL) emission at a wavelength of 792 nm, corresponding to the  $11H$  transition in the WW (i.e.,  $e_{\text{WW}}^1-hh_{\text{WW}}^1$ ). The other feature observed at low excitation intensity was the much weaker  $11L$  transition also related to the WW (i.e.,  $e_{\text{WW}}^1-lh_{\text{WW}}^1$ ). However, at 77 K, and at the highest CW excitation intensity used ( $\approx 10$  W/cm<sup>2</sup> at  $\lambda_{\text{ex}}=514.5$  nm), the  $\text{Al}_x\text{Ga}_{1-x}\text{As}$  gap transition (from the epilayers) could be observed, and also a peak (at about 730 nm) more than  $10^5$  times weaker than the  $11H$ : see Fig. 3(a), curve *i*. The photocreated electrons captured by the NW resonantly tunnel to the WW through the miniband and then relax to the  $e_{\text{WW}}^1$  state to give rise to the  $11H$  transition in the WW. The predominance of the  $11H$  peak in the WW over the electron miniband (em)- $hh_{\text{NW}}^1$  transition in the NW is a direct consequence of faster resonant tunneling. Oberli *et al.* and Deveaud measured resonant-tunneling time smaller than 10 ps,<sup>6,7</sup> about 100 times shorter than the typical interband relaxation time. The energy of the weak peak at  $\sim 730$  nm corresponds to the bottom of the electron miniband to the  $hh_{\text{WW}}^1$  level in agreement with miniband states retaining their first-excited-states symmetry in the WW region. Moreover, this weak peak obtained with the ADQWSL is clearly redshifted with respect to the  $11H$  transition in the NW of the corresponding isolated SQW as shown in curve *ii*. Curve *ii* was obtained with an equivalent sample having only one WW and one NW iso-

lated from each other with a 50-nm barrier, in which case the tunneling from the NW to the WW can be neglected, and the  $11H$  peak from the WW and the  $11H$  peak from the NW have the same order of magnitude. Curve *iii*, which shows the PL excitation (PLE) spectrum of the uncoupled NW and WW sample (monitoring the intensity of the  $11H$  peak in the WW), displays the interband transitions in the WW which were used together with the growth parameters to determine more accurately the energy levels of the constituent wells, and hence the energies of the expected miniband transitions in the ADQWSL structure: see the horizontal solid lines at the top of Fig. 3(a). The endpoint of the predicted miniband transitions nicely extrapolate to the peaks of the PLE spectrum obtained with the ADQWSL sample in curve *iv*. The smooth absorption onset characteristic of SL's, and centered near the position of the corresponding transitions in the isolated wells observed in curve *iv* in PLE, were also observed in photovoltaic (PV) experiments.

The PV results obtained between 0 and  $-3.0$  V every  $-0.5$  V with the ADQWSL sample (in a Schottky diode configuration) are shown in Fig. 3(b), which also reproduces the two PLE spectra of Fig. 3(a) for comparison purposes. The 0-V bias PV spectrum is very similar to the PLE spectrum obtained with the ADQWSL, as they

are both a measure of the absorption near the flat band condition. The transitions which involve uncoupled energy levels (e.g.,  $11H$  and  $11L$  in the WW) do not suffer from the Wannier-Stark effect, and are only shifted by the quantum-confined Stark effect. The measured Stark shift of the  $11H$  transition in the WW is about 1 meV, slightly smaller than the 2-meV shift calculated neglecting exciton effects. The Wannier-Stark effect on the miniband transitions can be followed [see center region of Fig. 3(b)] as the electric field increases from 0 V toward the  $-3.0$ -V spectrum. Although a precise identification of the Wannier-Stark ladders is difficult because of the convolution of the electron miniband transitions and the light-hole miniband transitions, the spectra tend to evolve from one which resembles the PLE spectrum obtained with the ADQWSL, toward one characteristic of localized states as in the case of the PLE spectrum obtained with the isolated SQW's. Moreover, the sharp feature at  $\lambda \approx 705$  nm in the 0-V spectrum starts to develop a higher-energy shoulder at an applied voltage of about  $-1.5$  V, corresponding to an electric field of 24 kV/cm. This confirms experimentally that at electric-field strengths above about 20 kV/cm the miniband of the ADQWSL is broken into Stark ladders.

Similar miniband transitions were also observed with a second sample ( $X=0.357$ ; 30 periods of  $L_{NW}=1.63$  nm and  $L_{WW}=6.3$  nm, and  $d=3.4$  nm), which has  $e_1^{NW}$  and  $e_2^{WW}$  off-resonance by 5 meV, and a miniband width of 64 meV. PLE and electroreflectance (ER) spectra are shown in Fig. 4 together with the expected electron miniband transitions. Features are observed in the PLE spectrum at the  $\Gamma$  and  $\Pi$  points of the miniband transitions, similarly to sample 1, but the smooth (inverse cosine) change in the density of state is better reflected in the spectrum because of the wider miniband (see for instance the  $em-hh_1^{NW}$  transition with the  $\Gamma$  point at  $\lambda=729$  nm, and the  $\Pi$  point at 702 nm). The  $em-hh_1^{NW}$  transition is better observed in the ER spectra, which show typical sharp derivativelike features for the GaAs and  $Al_xGa_{1-x}As$  gaps, and for the  $11H$  and  $11L$  transitions in the WW.

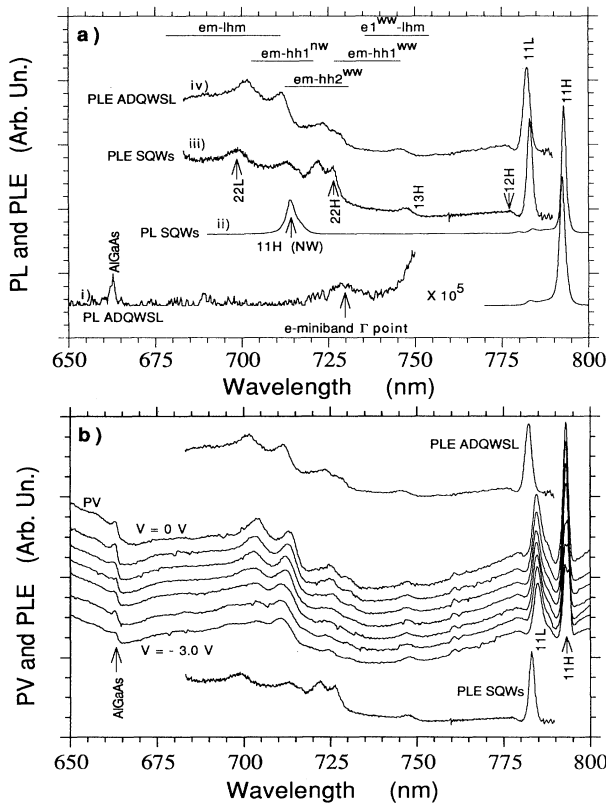


FIG. 3. (a) PL and PLE spectra obtained at 77 K with ADQWSL sample 1 (curves *i* and *iv*), and with a corresponding sample having only one WW and one NW isolated from each other with a 50-nm barrier in curves *ii* and *iii*; and the expected miniband transitions. (b) PV spectra obtained at 77 K with ADQWSL sample 1, compared with the PLE spectra of (a).

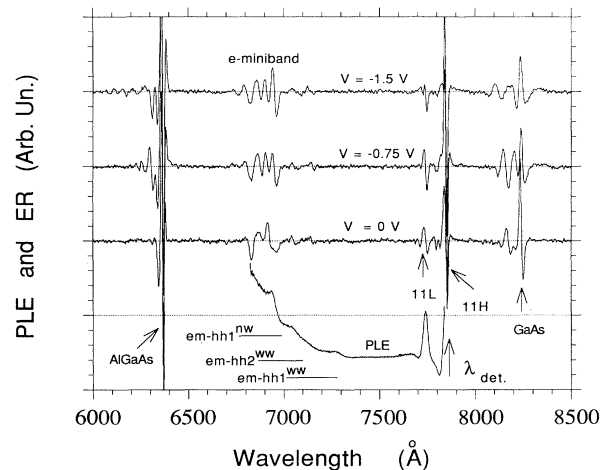


FIG. 4. PLE spectrum and ER results obtained at 77 K with ADQWSL sample 2.

The electric-field-dependent oscillations in the ER signal at the  $em-hh_1^{NW}$  energies are attributed to transitions involving the Wannier-Stark ladders of the collapsing miniband.

In summary, we have demonstrated the idea of miniband formation in ADQWSL structures built with a narrow well having a single bound electron state resonant with an excited state of a wider well. We have demonstrated with optical experiments how this breed of semiconductor heterostructure uniquely combines the sharp optical properties of MQW's and the miniband properties of SL's. We have miniband-engineered samples which achieved miniband formation through the extended states resulting from the resonant  $e_1^{NW}$  and  $e_2^{WW}$ , while keeping

localized ground states in the WW. As the energy difference between the discrete ground state and the upper miniband is tunable through the choice of the barrier height, the ADQWSL structure should have important practical applications for infrared detection or PL up-conversion<sup>14</sup> using tailored intersubband transitions linking the localized and miniband states. We are currently doing infrared and time-resolved experiments to better understand the intersubband transitions and the dynamics of the carriers in the ADQWSL.

One of us (S.F.) would like to acknowledge the Natural Science and Engineering Research Council of Canada (NSERC) for financial support.

\*Present address: Hughes Research Laboratories, 3011 Malibu Canyon Road, Malibu, CA 90265.

<sup>1</sup>For a recent review of semiconductor quantum heterostructures, see L. L. Chang and L. Esaki, *Phys. Today* **45** (10), 36 (1992).

<sup>2</sup>G. Hasnain, B. F. Levine, D. L. Sivco, and A. Y. Cho, *Appl. Phys. Lett.* **56**, 770 (1990); E. R. Brown, K. A. McIntosh, F. W. Smith, and M. J. Manfra, *Appl. Phys. Lett.* **62**, 1513 (1993).

<sup>3</sup>S. Fafard, Y. H. Zhang, and J. L. Merz, *Bull. Am. Phys. Soc.* **38**, 703 (1993).

<sup>4</sup>G. T. Einevoll and L. J. Sham, *Phys. Rev. B* **46**, 7787 (1992).

<sup>5</sup>L. S. Yu, S. S. Li, and P. Ho, *Appl. Phys. Lett.* **59**, 2712 (1991).

<sup>6</sup>D. Y. Oberli *et al.*, *Phys. Rev. B* **40**, 3028 (1989).

<sup>7</sup>B. Deveaud, in *Proceedings of the 20th International Conference on the Physics of Semiconductors, Thessaloniki, 1990*, edited by E. M. Anastassakis and J. D. Joannopoulos (World Scientific, Singapore, 1990), p. 1021; J. Shah, K. Leo, D. Y. Oberli, T. C. Damen, D. A. B. Miller, and J. P. Gordon, *ibid.*, p. 1222.

<sup>8</sup>Ph. Roussignol, A. Vinattieri, L. Carraresi, M. Colocci, and A. Fasolino, *Phys. Rev. B* **44**, 8873 (1991).

<sup>9</sup>D. H. Levi, D. R. Wake, M. V. Klein, S. Kumar, and H. Morkoç, *Phys. Rev. B* **45**, 4274 (1992).

<sup>10</sup>E. E. Mendez, F. Agulló-Rueda, and J. M. Hong, *Phys. Rev. Lett.* **60**, 2426 (1988); E. E. Mendez and F. Agulló-Rueda, *J. Lumin.* **44**, 223 (1989); E. E. Mendez, *Proceedings of the 20th International Conference on the Physics of Semiconductors* (Ref. 7), p. 1206; E. E. Mendez and G. Bastard, *Phys. Today* **46** (6), 34 (1993).

<sup>11</sup>Y. J. Mii, R. P. G. Karunasiri, K. L. Wang, M. Chen, and P. F. Yuh, *Appl. Phys. Lett.* **56**, 1986 (1990).

<sup>12</sup>D. F. Nelson, R. C. Miller, and D. A. Kleinman, *Phys. Rev. B* **35**, 7770 (1987); U. Rössler, *Solid State Commun.* **65**, 1279 (1988).

<sup>13</sup>Equation (2) of the following reference is particularly useful for deriving Eqs. (1): S. Fafard, E. Fortin, and A. P. Roth, *Can. J. Phys.* **69**, 346 (1991).

<sup>14</sup>P. Vagos, P. Boucaud, F. H. Julien, and J.-M. Lourtioz, *Phys. Rev. Lett.* **70**, 1018 (1993).